Chapter 26

Methods for Using a Genetically Encoded Fluorescent Biosensor to Monitor Nuclear NAD+

Michael S. Cohen, Melissa L. Stewart, Richard H. Goodman, and Xiaolu A. Cambronne

Abstract

Free nicotinamide adenine dinucleotide (NAD^+) serves as substrate for NAD^+-consuming enzymes. As such, the local concentration of free NAD^+ can influence enzymatic activities. Here we describe methods for using a fluorescent, genetically-encoded sensor to measure subcellular NAD^+ concentrations. We also include a discussion of the limitations and potential applications for the current sensor. Presented in this chapter are (1) guidelines for calibrating instrumentation and experimental setups using a bead-based method, (2) instructions for incorporating required controls and properly performing ratiometric measurements in cells, and (3) descriptions of how to evaluate relative and quantitative fluctuations using appropriate statistical methods for ratio-of-ratio measurements.

Key words NAD^+, Nicotinamide adenine dinucleotide, Biosensor, Metabolite, Fluorescent sensor, Circularly permuted fluorescent protein, ARTD, PARP

1 Introduction

The key advantage of using a sensor to measure oxidized β-nicotinamide adenine dinucleotide (NAD^+) is its ability to provide measurements of free NAD^+ in relevant physiological contexts. Because NAD^+ can have distinct roles in different compartments and additionally be regulated on a subcellular level, it is important to assess and differentiate its local concentrations. Whole-cell measurements from lysates are at a disadvantage in this regard because compartmentalized information is typically lost and it is technically challenging to differentiate free and bound NAD^+. A genetically encoded sensor can be (1) subcellularly localized or expression-restricted to specific cell or tissue types, (2) used on live cells for dynamic monitoring, and (3) used in context to distinguish free NAD^+, which is the fraction relevant to cellular signaling.

Paul Chang (ed.), *ADP-ribosylation and NAD+ Utilizing Enzymes: Methods and Protocols*, Methods in Molecular Biology, vol. 1813, https://doi.org/10.1007/978-1-4939-8588-3_26, © Springer Science+Business Media, LLC, part of Springer Nature 2018

NAD^+ has a well-known role as an electron acceptor in reductive and oxidative (redox) reactions. In addition, NAD^+ is utilized as a substrate for NAD^+-consuming enzymes, such as PARP (also known as ARTD) family members [1, reviewed 3–5] and sirtuins [2, reviewed in 3–5]. To mediate enzymatic ADP-ribosylation, PARP/ARTD family members transfer the ADP-ribose unit from NAD^+ to target proteins and release nicotinamide. As such, one NAD^+ molecule is consumed for each posttranslational ADP-ribosylation modification. The activities of PARP/ARTD family members thus rely on the local availability of free NAD^+. We describe here an approach to directly monitor this free NAD^+ pool in specific subcellular compartments.

In cells, a significant proportion of NAD(H) exists as a protein-bound fraction that is predominantly engaged in redox reactions [6–8]. Importantly, steady-state levels of this NAD(H) pool are not thought to fluctuate due to the nonconsuming nature of redox reactions. In contrast, there exists a free NAD^+ fraction—the fraction available for consumption by NAD^+-consuming enzymes—which is susceptible to steady-state changes. This free pool is estimated to comprise ~30% of total NAD content [8]. Total NAD^+ measurements from lysates typically represent a combination of the bound and free fraction. Therefore, data obtained from this approach may not accurately represent the amount of free NAD^+ available to NAD^+-consuming enzymes.

Free NAD^+ is further compartmentalized subcellularly, and its levels may be differentially regulated among cell types and tissues. The enzymes regulating NAD^+ biosynthesis and consumption localize to specific subcellular compartments and have varying expression levels in different cell types [4, 5, 9–13]. This provides a mechanism for how steady-state, free NAD^+ levels are differentially regulated within and among cells [14–20]. The subcellular compartmentalization of NAD^+ further highlights a limitation of whole-cell, lysate measurements for monitoring the specific pool of NAD^+ available to a particular NAD^+-consuming enzyme.

Unlike NADH, NAD^+ does not have intrinsic fluorescence to facilitate its detection in cells. NADH measurements or measurements of the NADH/NAD^+ ratio are unreliable indicators of free intracellular NAD^+ concentrations because of the high ratio of free NAD^+ to NADH [8]. Instead, fluctuations in NADH or ratiometric NADH/NAD^+ sensors predominantly reflect cellular redox state. In the nucleocytoplasm, the ratio of free NAD^+ to NADH is estimated at ~700:1 and in the mitochondria ~7:1 [8]. Furthermore, current ratiometric NADH/NAD^+ sensors are prone to saturation for NAD^+ at physiological concentrations, in effect being overly sensitive for most *in-cell* NAD^+ measurements [21–23]. Magnetic resonance scanning is helpful for in vivo patient diagnosis and can distinguish NAD^+ from NADH, but it is limited with regard to subcellular resolution and distinguishing the bound from free

fractions [24]. Lastly, while indirect readouts such as the PARAPLAY assay have been extremely informative [15], we sought to develop a quantitative approach for direct detection of NAD+ in intact cells. The advance we have developed is a genetically encoded fluorescent sensor for free NAD+ that can be localized to specific subcellular compartments for real-time, direct measurements in live cells [17].

The NAD+ sensor is based on a circularly permutated fluorescent protein, cpVenus, cleaved between its original amino acids 144 and 145 to position new N- and C-termini in close proximity to the central fluorophore; the original termini were joined with a small linker [25, 26]. Circularly permutated fluorescent proteins have been used in a variety of single-fluorescent protein sensors by connecting the fluorescent protein to a peptide-binding domain for the target molecule of interest [reviewed in 27, 28]. In this case, we attached a specific NAD+-binding pocket modeled after the NAD+-binding domain from LigA *E. faecalis* to the new termini and engineered it to reversibly bind and not consume NAD+ (*see* Fig. 1) [17, 29, 30]. The sensor was further confirmed to specifically recognize free NAD+ (and not NADH or other analogous molecules) and was optimized for its recognition of NAD+ within the physiological range [17]. This general design for a single-fluorescent protein sensor is analogous to what has been described by Tsien and Miyawaki groups, in their pioneering calcium sensors [25, 31], and also what has been subsequently utilized in many other single-fluorescent protein biosensor designs, including those used for the GCaMP and GECO sensor series and the NADH/NAD+ sensors [21–23, 32–35]. Because the sensor is genetically encoded, we can incorporate subcellular localization sequences to target the sensor to specific subcellular compartments for local NAD+ measurements [17].

The NAD+ sensor has a major fluorescence peak that is excitable at 488 nm and emits at ~520 nm and a weaker secondary peak that is excitable at 405 nm and emits at ~510 nm [17]. The fluorescence from 488 nm excitation decreases in the presence of free NAD+ and represents the readout of NAD+ concentration. In contrast, the 405 nm fluorescence is not significantly altered by NAD+ concentration, tracks with the expression level of the sensor, and can be used to normalize for varying sensor concentrations in cells [17]. Thus, the sensor uses ratiometric 488/405 nm measurements to follow how NAD+ fluctuates in cells. This type of ratiometric measurement is similarly used by other sensors and

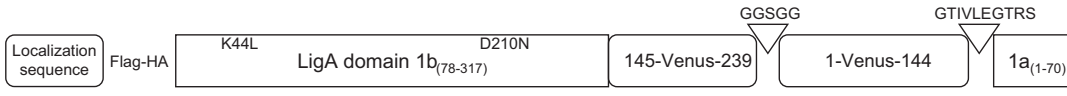

Fig. 1 Schematic of NAD+ sensor

probes, such as Pericam, HyPer, and Fura-2, to normalize for probe or sensor concentration or expression level [31, 36, 37]. There is an inverse relationship between the 488 nm fluorescence from the sensor and local NAD^+ concentrations; when NAD^+ concentrations are increased, the sensor's 488/405 nm fluorescence dims, and when NAD^+ concentrations are lowered, this fluorescence ratio brightens.

An additional important control for all experiments is cpVenus alone, without the NAD^+-binding pocket. NAD^+ has no measurable effect on the 488/405 nm fluorescence of cpVenus in vitro. However, we found that pH influences the fluorescence intensities of both the sensor and cpVenus control to comparable degrees between pH 6.6 and 8.0 [17]. Thus, a parallel analysis of fluorescent changes in cpVenus is required for normalization of pH effects or any other non-specific changes in fluorescence.

This leads us to a discussion of the current limitations of the sensor. One of the limitations is its pH dependency, most likely related to the pKa of cpVenus that was used in construction of the sensor. Nevertheless, because cpVenus fluorescence is similarly affected by pH, one can use cpVenus 488/405 nm fluorescence to normalize for NAD^+-independent changes in the sensor. We found that normalizing with cpVenus across this pH range minimizes the influence of pH and exposes the NAD^+-dependent changes [17]; similar strategies have been previously successful [38, 39]. The limitation is that these dual measurements require parallel analysis of the sensor and cpVenus under similar experimental conditions. Nevertheless, if it is initially established that pH does not change over the course of an experiment, NAD^+ fluctuations can be monitored in single cells with the sensor's 488 nm fluorescence.

The presence of high NAD^+ concentrations maximally lowers the 488 nm fluorescence by ~50% but does not eliminate it. Thus, cellular conditions where fluorescence is eliminated both from the sensor and cpVenus—e.g., pH $\leq$6.5 or exogenous H_2O_2 treatment—are incompatible with measurements. Only a few subcellular compartments—namely, the *trans*-Golgi network, secretory granules, endosomes, and lysosomes—exhibit pH <6.5, however. Most intracellular compartments fall within the measurable pH range, including the nucleus, cytosol, mitochondria, peroxisomes, endoplasmic reticulum, and *cis*-Golgi network [reviewed in 40].

Another limitation of the sensor is that this version may not be sufficiently sensitive to reliably detect all modest NAD^+ changes; this sensitivity may also depend on how well the instrumentation can monitor its fluorescence.

We describe here methods for expressing the sensor and cpVenus control in mammalian cells, as well as for generating a standard curve to quantify nuclear measurements using sensor-coated and cpVenus-coated beads and a buffered NAD^+ stock (*see* Materials). We have found that this bead-based approach coupled to flow

cytometry is amenable for quantifying depleted NAD^+ concentrations, as could be expected in scenarios with unbalanced rates of NAD^+ consumption.

2 Materials

2.1 Plasmid DNA, Cell Culture, Transfection, and Small-Molecule Treatments

1. Plasmid DNA: Follow manufacturer's instructions for column-prep plasmid maxiprep. Resuspend plasmid DNA in 10 mM Tris pH 8.0 at a concentration of 1 mg/mL.
2. HEK293T cells: Maintain and propagate in a humidified incubator at 37 °C in 5% CO_2, and routinely passage with sterile technique in a biosafety cabinet.
3. Complete DMEM growth media: DMEM, 10% fetal bovine serum, and 25 mM HEPES pH 7.4.
4. Complete MEM media for small-molecule treatments and analysis: MEM, 10% fetal bovine serum, and 25 mM HEPES pH 7.4.
5. Sterile water.
6. 2.5 M $CaCl_2$ stock.
7. 2× HBS pH 7.1: 40 mM HEPES, 10 mM KCl, 270 mM NaCl, 1.5 mM Na_2HPO_4, and 10 mM dextrose; adjust to pH 7.1 with NaOH and filter sterilize (*see* **Note 4**).
8. Lipofectamine 2000™.
9. Serum-free Opti-MEM™ media.
10. Inverted light microscope with phase contrast, a broad LED excitation source (Lumencor Sola SMII Light Engine), and fluorescence filter sets for 525 ± 25 nm.
11. PVDF low protein-binding filter syringe, 0.45 μm.
12. Puromycin: 10 mg/mL aliquoted stocks in sterile water can be store up to a year at −20 °C. Puromycin is freshly diluted in media prior to use.
13. FK866 (N-[4-(1-benzoyl-4-piperidinyl)butyl]-3-(3-pyridinyl)-2ε-propenamide): 50 mM stocks in DMSO, stored in aliquots at −20 °C. Immediately before use, serially dilute FK866 with complete MEM media to a final concentration of 10 nM.
14. Nicotinamide riboside chloride: freshly resuspend powder as a 200 mM stock solution in 10 mM citrate buffer pH 3, aliquot, and store at −20 °C for use within 2 weeks. Immediately before use, dilute the nicotinamide riboside stock to 500 μM in complete MEM media. An equivalent volume of citrate buffer is added to control cells.

2.2 Generation of Sensor-/cpVenus-Coated Beads

1. 0.5% NETN buffer: 20 mM Tris pH 7.4, 150 mM NaCl, 0.5% NP-40, 1 mM EDTA, and protease inhibitors. To make 40 mL of 0.5% NETN buffer, dissolve two EDTA-free protease inhibitor tablets (Sigma) into 36 mL ultrapure water. Add 800 μL of 1 M Tris pH 7.4, 1.2 mL of 5 M NaCl, 2 mL of 10% NP-40, and 80 μL of 0.5 mM EDTA pH 8. Assemble buffer and prechill the same day you plan to perform the cell lysis.
2. Anti-Flag M2 magnetic beads (Sigma); average diameter 50 μm.
3. Magnetic stand compatible with 1.5 mL snap-cap tubes and 15 mL conical tubes.

2.3 Buffered 50 mM NAD^+ Stock Solution

1. Assay buffer: 100 mM Tris pH 7.4 and 150 mM NaCl.
2. 50 mM NAD^+ stock: Resuspend 25 mg of NAD^+ (>99% pure, molecular weight 663.4 g/mol) in 500 μL of assay buffer. This buffer composition is important, as NAD^+ is unstable in phosphate buffers [41], and addition of salt helps maintain proper protein conformation when incubated with sensor or cpVenus proteins. Initially increase the pH with ~25 μL of 1 N NaOH to approximately pH 6.5. Then slowly add 0.1 N NaOH (~10 μL) to increase to pH 7.5. Mix well and use pH strips to confirm pH. Total volume is now approximately 535 μL. Add the remaining volume of buffer up to 753.6 μL total for a 50 mM stock. Mix well. Aliquot and store at −20 °C or −80 °C.

2.4 Ratiometric Fluorescent Measurements

1. Flow cytometer: BD LSR II™ (or similar) with filter set Violet-2A (e.g., 405 nm; Em. 525 ± 25 nm) and filter set FL 1-A (e.g., 488 nm, Em. 530 ± 15 nm).
2. FlowJo™ data analysis software (or similar).
3. 5 mL polypropylene round bottom tubes.

3 Methods

3.1 Expression of the Sensor and cpVenus Control in Mammalian Cells

The approach described below is generally accessible to a wide scientific audience and does not require a BL2-approved workspace, lentivirus helper plasmids, or viral packaging. However, it requires micrograms of maxi-prepped DNA. For some researchers, it may be more cost-effective to generate stably expressing cell lines via viral transduction. We briefly describe that protocol in Subheading 3.2. Once cells are either transiently or stably expressing the sensor, the researcher can advance directly to Subheading 3.3.

1. Begin with a healthy HEK293T cell culture that has been passaged at regular intervals. Prepare a total of 8 × 10 cm dishes, where 6×10^6 cells have been seeded for each 10 cm dish. Four of the dishes will be used for expressing and purifying the sensor, and the remaining four will be used for cpVenus (*see* **Note 1**).

2. The next day, confirm with light microscopy that HEK293T cells have attached and are evenly distributed. Following a standard calcium phosphate protocol, transfect high-quality maxi-prepped plasmid DNA expressing the sensor or cpVenus control (20 μg per dish) (*see* **Notes 2** and **3**). For simplicity, DNA stocks can be prepared at a concentration of 1 mg/mL.

   In summary, for each condition, combine the following together in a 50 mL conical tube and vortex to mix well: a total of 80 μg plasmid DNA, 3.52 mL of sterile water, and 400 μL of 2.5 M $CaCl_2$. While aerating the mixture with a 5 mL pipette, slowly add 4 mL of 2× HBS in a dropwise manner (*see* **Note 4**). This mixture is incubated for 15 min at room temperature before being added dropwise to cells, 2 mL of mixture per 10 cm plate.

3. Forty-eight hours post transfection, using an epifluorescence microscope with an inverted stage that can accommodate dishes confirms that the cells are expressing either sensor or cpVenus with a transfection efficiency >80%. Cells should fluoresce at ~520 nm after either broad excitation or with a 488 nm light source and are expected to express predominantly in the cytoplasm.

4. Proceed to the generation of sensor-coated beads. Alternatively, cell pellets can be collected, flash frozen in liquid nitrogen, and stored at -80 °C for up to several months.

3.2 Viral Transduction to Generate a Stably Expressed Cell Line

The section describes an alternative method for generating stably expressing sensor and cpVenus cell lines that can be expanded to obtain 4 × 10 cm dishes of cells or used for measurement, if generated using targeted versions of the sensor and cpVenus. This approach requires a biosafety level 2 (BL2)-approved workspace, and steps are performed in a biosafety cabinet, using sterile technique and reagents. Standard BL2 viral handling safety precautions must be followed and performed in a BL2-approved workspace. These versions of the sensor and cpVenus are encoded in lenti-compatible plasmids, and their expression is driven by a CMV promoter. Their coding sequences are followed by an internal ribosome entry site (IRES) and puromycin selection marker. We describe transfection with the Lipofectamine 2000™ reagent, but analogous approaches for introducing plasmids into mammalian cells work equally well. Co-transfection of the sensor plasmids with second-generation helper plasmids will produce infective lentiviral particles.

1. Begin with a healthy HEK293T cell culture that has been passaged at regular intervals. Split one million cells per well in a 6-well (35 mm) plate.

2. The next day, confirm with light microscopy that HEK293T cells have attached and are evenly distributed in the 35 mm

dish or well. Transfect these cells with Lipofectamine 2000™, following manufacturer's directions. Optimal transfections are achieved using high-quality, maxi-prepped plasmid DNA for the sensor/cpVenus and helper vectors.

In summary, for each well, we premix the sensor/cpVenus (2 μg) with the helper plasmids (2 μg) in a sterile 1.5 mL snap-cap tube (total DNA is 4 μg) and then mix in 200 μL of neural-pH serum-free Opti-MEM™ media. In a separate snap-cap tube, first dilute 10 μL of Lipofectamine 2000™ reagent into 200 μL of Opti-MEM™, and then transfer this Lipofectamine 2000™/Opti-MEM™ mixture to the DNA/Opti-MEM™ mixture. Vortex together to mix and incubate at room temperature for 20 min. After the incubation, add this mixture dropwise to the pre-seeded HEK293T cells.

3. After 4–6 h, gently remove media on cells and replace with fresh growth media.
4. Allow cells to express the sensor and cpVenus control from the transfected plasmids for 48–72 h. Confirm this expression and a >80% transfection efficiency with epifluorescence widefield microscopy. Successful viral packaging can often be observed at this point by a slightly round and swelling morphology of the packaging cell. Very gently transport your plate to and from the incubator, as the cells are liable to detach very easily at this stage.
5. Collect the virus-containing growth medium from the transfected cells between 48 and 72 h post transfection; do not disturb or collect the cell monolayer. Spin the virus-containing growth medium at 1500 × *g* for 5 min to pellet cellular debris. Carefully remove the supernatant without disturbing the pellet, and pass this supernatant through a low protein-binding 0.45 μm PVDF syringe filter. Approximately 1.5 mL of viral supernatant is typically recovered from 2 mL of media. Viral titer or infectivity units can be calculated at this point, if desired.
6. Trypsinize and count HEK293T cells from a healthy culture. Mix 500×10^3 cells with 0.5 mL of filtered viral supernatant in a 12-well plate. Add 0.5 mL of fresh growth media and incubate overnight.
7. The next day, gently remove viral supernatant and growth media from the transduced cells that are now adhered to the 12-well plate. Replace with fresh growth media.
8. After waiting 48 h to allow for expression of the puromycin resistance gene, trypsinize cells from the 12-well plate and replate in a 10 cm plate containing growth media with 1 μg/mL puromycin for selection of transduced cells. As a control, an untransduced 12-well plate of cells is also split into growth

media containing puromycin. The cells in this control should not survive the puromycin selection because they are not transduced, and in contrast the transduced cells should fluoresce green and proliferate under the same puromycin selection conditions.

9. Check cells undergoing puromycin selection daily. If there are a lot of unhealthy or unattached cells in the culture, gently wash away the debris from attached growing cells by removing the media and replacing with fresh growth media containing puromycin.
10. Cell lines should be expanded and grown under puromycin selection for a minimum of 1–2 weeks. At this point, cells can be frozen in 10% DMSO as freezer stocks for storage at −80 °C or in liquid nitrogen.

3.3 Generation of Sensor-Coated and cpVenus-Coated Beads

All steps are performed at 4 °C or on ice. Store sensor-coated beads at 4 °C, and do not freeze-thaw. We recommend using these beads the same day for best results. If stored in buffer with protease inhibitors, we have not noticed substantial differences for up to 3 days. We do not recommend using protein-coated beads that have been stored for over a week, due to the chance of proteolysis or denaturation.

1. On ice, remove growth media from 10 cm plate of cells, and collect cells in 5 mL of PBS per 10 cm plate with gentle scraping using a cell scraper. Pool cells from the same condition into a 50 mL conical tube.
2. To collect cells as a pellet, centrifuge tubes at 4 °C at 1000 × *g* for 5 min. Carefully remove and discard PBS supernatant from cells.
3. To extract the sensor and cpVenus proteins, lyse cells by resuspending them in 0.5% NETN buffer, and incubate suspension on ice for 10 min. Use 2.5 mL of buffer per 10 cm plate; for 4 × 10 cm plates, this volume is 10 mL.
4. Clarify the lysate by centrifugation at 12000 × *g* for 20 min at 4 °C (*see* **Note 5**).
5. While the lysates are spinning, prepare the anti-Flag magnetic beads with an average diameter of 50 μm. Use 20 μL of slurry per 10 cm dish. For eight dishes, we need 160 μL slurry of beads and therefore prepare 175 μL slurry to provide excess to account for any pipetting error. Use a cut tip or one with a wide orifice to pipette to a new 1.5 mL tube. Place the tube on a magnetic stand for 2 min, and wash beads twice with 0.5% NETN buffer. Resuspend the washed beads in 600 μL of 0.5% NETN, and distribute 300 μL of the resuspended beads into 2 × 15 mL conical tubes. Place conical tubes on magnetic stand at 4 °C until lysate is prepared.

6. Following centrifugation of the lysate, the sensor and cpVenus proteins will remain in the supernatant. Remove this supernatant to a new tube.
7. Quantitate the amount of total protein in the lysate obtained from each sample using a Bradford assay or similar (*see* **Note 6**). With this procedure, we typically obtain values between 2 and 5 mg/mL for total protein concentration in the lysate. Calculate the required volumes from each sample such that relative total protein concentration is normalized between samples (*see* **Note 7**).
8. The washed beads in the conical tubes have now been magnetically separated. Carefully remove the buffer, and resuspend beads with the appropriate volume of clarified lysate. Perform this step sequentially for the sensor and cpVenus so that the beads do not dry out when the buffer is removed.
9. Secure the cap on the conical tubes, and incubate beads with lysate for 2 h at 4 °C on a rotator. This step coats the beads with sensor and cpVenus protein (*see* Fig. 2 and **Note 8**).
10. After incubation, place conical tubes back on the magnetic stand to separate the beads that are now coated with either the sensor or cpVenus protein.
11. While keeping the tube on the stand, gently wash beads twice with 1 mL of 0.5% NETN buffer.
12. It is highly recommended to proceed directly to calibration on the same day that the beads are generated. However, if beads need to be saved for the next day, they can be stored in 0.5% NETN at 4 °C following the wash steps.

3.4 Analyzing Sensor-Coated and cpVenus-Coated Beads on Flow Cytometer

1. NAD^+ is acidic, and it must be prepared as a buffered stock prior to use and storage in solution. Instructions for preparing a buffered 50 mM NAD^+ stock are found in Subheading 2.3. Using the buffered NAD^+ stock, prepare 1 mL of 2× NAD^+ buffers 2 mM and 6 mM NAD^+ in assay buffer (100 mM Tris pH 7.4, 150 mM NaCl). Using assay buffer, serially dilute the 2 mM and 6 mM stocks to prepare the series of 2× NAD^+ concentrations for the calibration curve (*see* Table 1).
2. Place tubes on the magnetic stand, gently remove 0.5% NETN, and resuspend each set of sensor-coated and cpVenus-coated beads in 1.05 mL of assay buffer. Using a cut tip, distribute 100 μL of each of the bead suspension evenly into 10 × 1.5 mL tubes. As each tube will correspond to different NAD^+ assay conditions, label each tube appropriately.
3. Add 100 μL of the appropriate 2× NAD^+ buffer to each tube. Keep beads cold during this process.

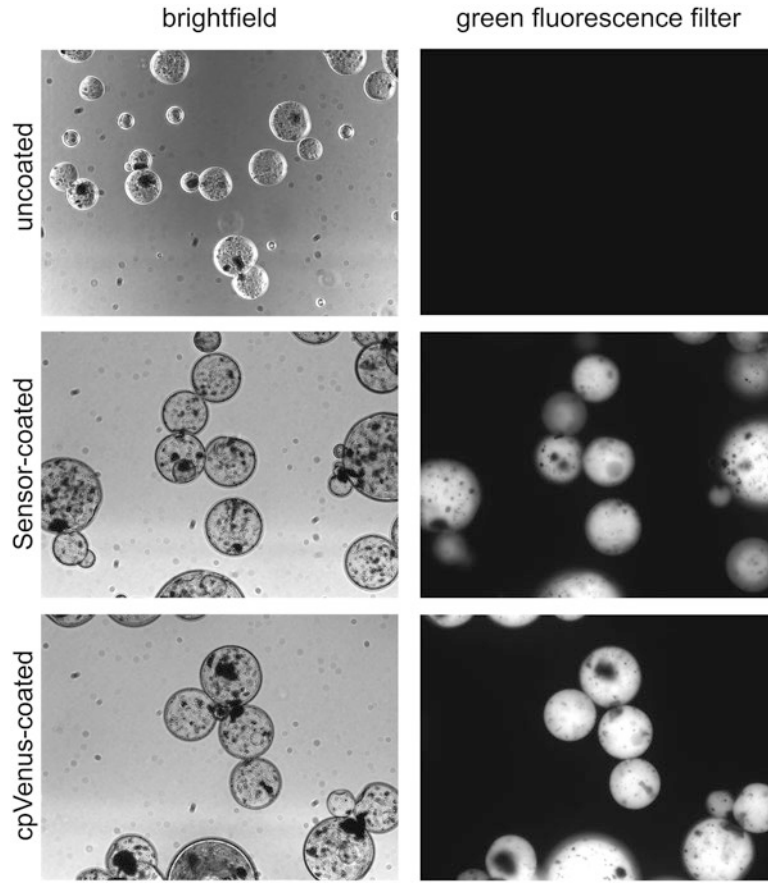

Fig. 2 Brightfield and epifluorescence images of uncoated (top), sensor-coated (middle), and cpVenus-coated (bottom) beads in suspension. Fluorescence was excited by an LED Sola SMII Light Engine, and emission was viewed through a 525 ± 25 nm filter, 30 ms exposure time

4. Ensure that the lasers on the flow cytometer have been warmed up and the detectors are stabilized. If needed, immediately prior to analysis, pass the resuspended beads through a 100 μm nylon mesh filter into the 5 mL round-bottom tube that will be used with the flow cytometer. This can help prevent clogging of the instrument from clumped or particularly large beads.
5. The first sample to run is uncoated beads (no fluorescence). This identifies a relatively uniform bead size (G1) based on forward and size scatter (*see* Fig. 3a). Generate a plot, and set the *x*-axis to FSC-A (log scale) and the *y*-axis to SSC-A (log scale) for forward and side scatter, respectively. Adjust voltages on the instrument to center the nonfluorescent bead popula-

Table 1
Conditions for bead-based calibration

cpVenus-coated beads		Sensor-coated beads		2× NAD^+ stock
Condition	**[NAD^+] μM**	**Condition**	**[NAD^+] μM**	**[NAD^+] μM**
1	0.01	11	0.01	0.02
2	0.1	12	0.1	0.2
3	1	13	1	2
4	3	14	3	6
5	10	15	10	20
6	30	16	30	60
7	100	17	100	200
8	300	18	300	600
9	1000	19	1000	2000
10	3000	20	3000	6000
21 uncoated beads (nonfluorescent)				

tion onto the lower left quadrant of this plot (*see* Fig. 3a and **Note 9**).

6. The sensor and cpVenus proteins externally coat the beads, and thus coated beads are expected to be irregularly shaped and have increased complexity, reflected by increased forward and side scatter values (G2).
7. To define fluorescent beads (FL), generate a second plot that displays events from G1 and G2. Set the *x*-axis to Violet-2A for the BD LSRII (e.g., 405 nm, filter set 525/50 nm) and the *y*-axis to FL1-A (e.g., 488 nm, filter set 530/30) (*see* **Notes 9** and **10**). Detectable fluorescence is defined by exclusion of the nonfluorescent beads (*see* Fig. 3a). Draw a gate (FL) to define the fluorescent beads above and to the right of the nonfluorescent bead sample.
8. Analyze the 20 total samples representing the effects of varying NAD^+ concentration on the fluorescence of cpVenus- or sensor-coated beads. Collect a minimum of 500 events from the FL gate, and save data from all events (*see* **Note 11**).

3.5 Generating a Standard Curve

1. Upload the data files (FCS files) obtained from the flow cytometer for post-capture analysis in FlowJo™ software or similar.
2. Open the file corresponding to the nonfluorescent beads, and define gates similarly as previously performed on the cytometer, with the FL gate being defined from the G1/G2 subsets.

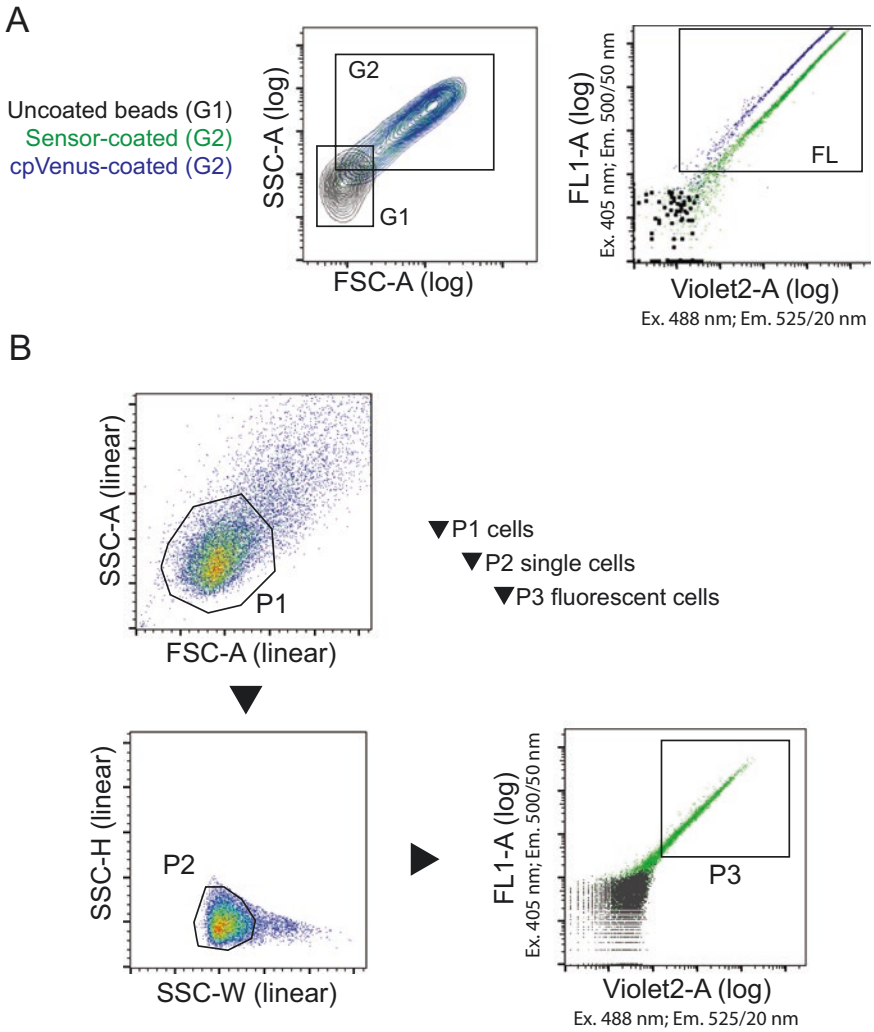

Fig. 3 (**a**) Example of flow cytometry analysis of sensor-coated (green) and cpVenus-coated (blue) beads, relative to uncoated beads (gray). Approximately 500 fluorescent events are analyzed in FL. (**b**) Hierarchical analysis of the size, granularity, and fluorescence of cells as measured through flow cytometry and represented as dot plots. Approximately 10×10^3 fluorescent cells are analyzed in P3. Nonfluorescent cells are overlaid in gray

Use exclusion of the nonfluorescent beads as boundaries for the FL population. We suggest viewing the data as a density plot or in pseudocolor. After defining these gates, drag these gate names to "All Samples" under the "group" heading in the workspace to ensure that identical gating is performed on all samples (*see* **Notes 12** and **13**).

3. To determine the fluorescence ratio 488 nm/405 nm per bead, select "derive parameters" under the "Tools" tab. Enter the "formula" by clicking "Insert Reference" to select the FL1-A value; click the ÷ key and "Insert Reference" to select Violet-2A (*see* **Note 14**).

4. Apply this "derived" parameter to "all samples." A histogram of the derived value should result in a defined peak. This represents the response of the sensor or cpVenus to the NAD^+ concentration, normalized for the amount of protein coating the bead. The geometric mean values of the derived parameter from the fluorescent FL group can be exported using the "Table Editor" function (*see* **Note 15**).
5. Divide the geometric mean of the sensor by the geometric mean of cpVenus for each NAD^+ concentration. We refer to this value as "the ratio of ratios" (*see* Table 2). The 488/405 nm fluorescence of cpVenus should not dramatically change across these conditions, and it is used in the denominator to normalize for any experimental technicalities that may non-specifically alter fluorescence. This can include slight pH differences across samples. If the NAD^+ stock is not sufficiently buffered, the cpVenus values will also trend as a decrease with its addition.
6. To obtain the standard curve, plot the ratio-of-ratio values in the *y*-axis against the log μM on the *x*-axis (*see* Fig. 4). This is expected to yield a sigmoidal curve and represents one replicate. Additional replicates can provide 95% confidence intervals for the curve.

Table 2
Example of ratio-of-ratio calculations for calibration curve

	Geo. mean 488/405 nm			Ratio of ratios
NAD^+ μM	cpVenus	Sensor	Log [NAD^+] μM	$(Sensor_{488/405nm})/(cpVenus_{488/405nm})$
0.01	5.18	1.95	−2.00	0.376
0.1	5.19	1.98	−1.00	0.382
1	5.2	1.97	0.00	0.379
3	5.09	1.93	0.48	0.379
10	5.12	1.84	1.00	0.359
30	5.17	1.75	1.48	0.338
100	5.17	1.53	2.00	0.296
300	4.97	1.33	2.48	0.268
1000	5.08	1.14	3.00	0.224
3000	5.08	1.01	3.48	0.199

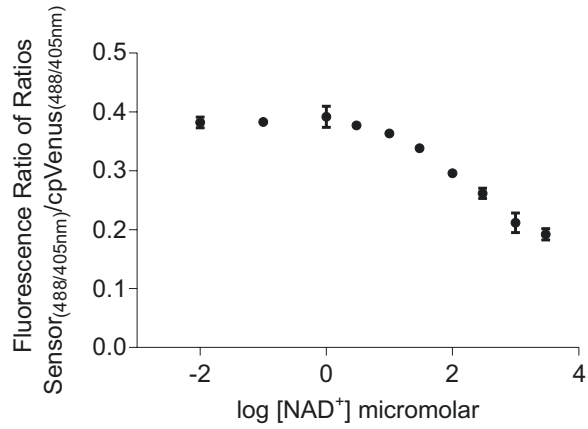

Fig. 4 Fluorescence data obtained with sensor- and cpVenus-coated beads, graphed against the log of NAD^+ concentrations. Mean ± SD, $n = 2$

3.6 Nuclear Expression of the Sensor in Cells Using Transient Transfection

To obtain measurements for intracellular NAD^+, the localized sensor and cpVenus control need to be expressed in your cell of interest. Because the presence of NAD^+ only decreases but doesn't eliminate the sensor's fluorescence, monitoring fluorescence and confirming nuclear localization of the sensor and cpVenus should be straightforward using fluorescence microscopy. The expression level of both the sensor and cpVenus can be normalized by the fluorescence at ~515 nm, following excitation at 405 nm; thus with sufficient sample size, measurements can be obtained from transiently transfected cells or non-clonal lines. Here we describe a basic protocol for examining NAD^+ depletion and increases in the nuclei of transiently transfected HEK293T cells (*see* **Note 16**).

1. Day 0: Starting with a healthy HEK293T cell culture, seed 5×10^5 cells in a 35 mm well. For this protocol, a minimum of 6 × 35 mm dishes or a 6-well plate is required, plus an extra well as an untransfected, nonfluorescent control for the flow cytometry data capture (*see* Table 3).
2. Day 1: The next day the cells are ready for transfection after confirming with light microscopy that they have adhered and are evenly distributed, ~30–50% confluent.
3. Under sterile conditions, and following manufacturer's directions, transfect 2 μg of nuclear cpVenus or nuclear sensor plasmid DNA using 5 μL of Lipofectamine 2000™ in 400 μL total of serum-free Opti-MEM™ media per well (*see* **Notes 17** and **18**).

   First prepare and vortex to mix well a master mix of 1.2 mL Opti-MEM™ media and 30 μL of Lipofectamine 2000™. Meanwhile, in separate tubes, dilute and vortex to mix well 6 μg of each plasmid DNA (nuclear cpVenus or sensor) in 600 μL of Opti-MEM™ media. Add 600 μL of the Lipofectamine 2000™/Opti-MEM™ mixture to each of the tubes containing

Table 3

Suggested experimental conditions for assessing NAD⁺ sensor changes in cells

Condition	Transfected plasmid	Treatment
1 *Nonfluorescent control*	–	–
2	Nuclear cpVenus	–
3	Nuclear sensor	–
4	Nuclear cpVenus	10 nM FK866, 6–8 h
5	Nuclear sensor	10 nM FK866, 6–8 h
6	Nuclear cpVenus	500 μM nicotinamide riboside, 24 h
7	Nuclear sensor	500 μM nicotinamide riboside, 24 h

FK866 is a specific inhibitor of nicotinamide phosphoribosyltransferase (NAMPT), the rate-limiting enzyme in the NAD⁺ salvage biosynthesis pathway that generates nicotinamide mononucleotide (NMN). NMN is a direct precursor for intracellular NAD⁺ Treatment with exogenous nicotinamide riboside can also influence steady-state NAD⁺ levels through NMN. Nicotinamide riboside serves as substrate for nicotinamide riboside kinase (NRK) to synthesize NMN

diluted plasmid DNA. Vortex to mix. Incubate for 20 min at room temperature. Add 400 μL of each transfection mixture to 3 × 35 mm wells.

4. Day 2: After allowing cells ~20–24 h to express the plasmid, use fluorescent microscopy to confirm nuclear expression of the sensor and cpVenus. Transfected cells should fluoresce green and localize to the nucleus (*see* **Note 19**).

3.7 Small-Molecule Cell Treatments

After confirmation of a successful transfection, cells are now ready for experimental treatment conditions 24 h post transfection. Here, we will use FK866 and nicotinamide riboside treatments to deplete or increase, respectively, nuclear NAD⁺ concentrations (*see* Table 3).

1. Serially dilute FK866 in complete MEM to a final concentration of 10 nM (5 mL). Separately, also prepare 500 μM nicotinamide riboside in complete MEM (5 mL) (*see* Table 3, **Note 20**, and Subheading 2).
2. Gently remove growth media completely from each well, and carefully replace with 2 mL complete MEM media containing

either buffer, 10 nM FK866, or 500 μM nicotinamide riboside.

3. Return to incubator for 4–16 h for nuclear FK866 treatment (*see* **Note 21**) and 16–24 h for nicotinamide riboside treatment.

3.8 Obtaining Nuclear Ratio-of-Ratio Measurements in Cells

1. Cells are ready for flow cytometry analysis at 48 h post transfection and 4–24 h after treatment (*see* **Note 22**). The time taken to prepare cells for flow cytometry analysis must be within 5 and 10 min from start to finish due to the analysis being performed on live cells out of the incubator. If you have more samples than can be handled within this timeframe, trypsinize, collect cells, and analyze in small batches (i.e., one 6-well plate at a time). The media used to resuspend cells (complete MEM growth media) must be made fresh such that it is within near-neutral pH. If it contains phenol red, the medium should be orange-red in color without any traces of pink or magenta. Ideally media is made immediately before cell collection. Media that is not near-neutral pH is unable to sufficiently buffer the cell suspension for the duration of the flow analysis (*see* **Notes 23** and **24**).
2. Prepare and label flow cytometry sample tubes on ice. Remove growth media from cells and gently wash 1× with PBS.
3. Add 100 μL of 0.05% EDTA-trypsin to each well of cells, and incubate at 37 °C until you can easily see cells come off the plate (approximately 3–5 min).
4. Add 400 μL freshly prepared complete MEM media to each well to quench the trypsin. Triturate with a 1 mL pipette tip to obtain single-cell suspension, and immediately transfer to a labeled sample tube on ice.
5. Prepare the flow cytometer similarly to what had been described for evaluating the beads. Use the untransfected control cells to adjust voltages to center the cells on a forward and side scatter plot; the *x*-axis is set to *linear* FSC-A, and the *y*-axis is set to *linear* SSC-A (*see* Fig. 3b). To identify the relatively uniform HEK293T cell size, adjust voltages on the instrument to center the population (*see* **Note 25**). Draw a gate to define this population as P1 (*see* Fig. 3b).
6. To select for individual cells (P2) and minimize evaluation of cells that have remained clumped together, generate a new plot for doublet exclusion as evaluated by wider widths. Select the P1 population for viewing, and set the *x*-axis to linear SSC-W and the *y*-axis to linear SSC-H. Draw the gate (P2) around the population on the left (*see* Fig. 3b).
7. To define the fluorescent cells (P3), generate a third plot that displays events from P2. Set the *x*-axis to log Violet-2A for the

BD LSRII (e.g., 405 nm, filter set 525/50 nm) and the *y*-axis to log FL1-A (e.g., 488 nm, filter set 530/30). The P3 population is derived from the P2 population and is defined by exclusion of the nonfluorescent cells (*see* Fig. 3b). Draw the P3 gate to the right and above the cell population observed in the untransfected control sample, ensuring that you do not include any events in this P3 gate (*see* **Note 26**).

8. After setting up these gates, you are now ready to evaluate the remaining samples. Each batch of samples to be analyzed should be completed within 15–20 min. It is necessary to collect at least 1×10^4 cells in P3 to rigorously evaluate the fluorescence of each sensor or cpVenus population. Save data from all events, and ensure that collected data includes fluorescence following 488 nm excitation at ~525 ± 25 nm and fluorescence following 405 nm excitation at ~515 ± 10 nm.
9. Perform a post-capture analysis with the data using FlowJo software, or similar, to obtain the geometric mean of the 488/405 nm fluorescence ratio from each cell in P3. This is done with the derived parameter function, akin to what was described for analyzing coated-bead fluorescence in Subheading 3.5.
10. For each condition (control, 10 nM FK866, or 500 μM nicotinamide riboside), divide the geometric mean of the 488/405 nm ratio of the sensor by the geometric mean of the 488/405 nm ratio of cpVenus. This is a normalization step that accounts for any non-specific changes independent of NAD^+ that may have influenced fluorescence intensities during the experiment (*see* Table 4).
11. Interpolate this value onto the standard curve to obtain values for nuclear NAD^+ concentrations under each condition. Confidence intervals are obtained from the curve.

3.9 REML Statistics Compared to Control to Evaluate Significance of Relative Changes

It is also possible to evaluate relative changes without generating a standard curve by comparing the change in the treated conditions relative to the untreated samples.

1. We begin by dividing the geometric mean 488/405 fluorescence value for the sensor by the corresponding value for the cpVenus control subjected to the same condition as described above (*see* Table 4).
2. We next use this normalized value to compare the treated condition to the control condition. This is performed by dividing treated normalized value by the value of normalized untreated cells. Because the sensor's fluorescence is inversely proportional to NAD^+ concentrations, it is expected that the sensor's fluorescence will increase in brightness with FK866 treatment

Table 4

Measuring relative changes with the nuclear sensor

Treatment	Nuclear sensor	Nuclear cpVenus	Ratio of ratios $Sensor_{(488/405nm)}$/ $cpVenus_{(488/405nm)}$	Relative change (treated/untreated)
0 nM FK866	0.93	3.00	*0.93/3.00* = 0.31	
10 nM FK866, 7 h	1.14	2.94	*1.14/2.94* = 0.39	*0.39/0.31* = **1.25**
Buffer	1.01	3.13	*1.01/3.13* = 0.32	
500 μM nicotinamide riboside, 24 h	0.91	3.34	*0.91/3.34* = 0.27	*0.27/0.32* = **0.84**

Steady-state NAD^+ levels are depleted following inhibition of its biosynthetic pathway with FK866 treatment. This is indicated by a ratio >1 when treated conditions are compared to control. Increases in steady-state NAD^+ levels are indicated by a ratio <1

and decrease in brightness with nicotinamide riboside treatment, compared to the untreated sensor. A relative increase in fluorescence is denoted by a value >1; a relative decrease in fluorescence will result in a value <1 (*see* Table 4).

3. To estimate the reliability of the experimental results and evaluate the likelihood that any observed fluorescence changes occurred by chance, we recommend analyzing the data using a mixed-effect model in which the experimental replicate is regarded as a random factor and the selective conditions of treated/control and sensor/cpVenus are both considered as fixed factors. This approach is most appropriate for evaluating the ratio of ratios, compared to other statistical evaluations, e.g., t-tests, and requires biological triplicates.
4. To stabilize variance and limit the impact of outliers, we first log transform the geometric mean fluorescence intensity value for 488/405 nm. The requirement for this transformation is based on our observations that the untransformed data violates the model's assumptions of normality of the error distribution and homogeneity of error variances; log-transformed data showed no such violations.
5. We estimate variance by performing a residual maximum likelihood (REML) analysis. This is performed using the 488 nm/405 nm geometric mean values for each experimental condition and requires a minimum of three biological replicates for statistical analysis. The *p*-value obtained for the interaction between the treated and control sensors, compared to the treated and untreated cpVenus, represents the *p*-value for the experimental replicates.

4 Notes

1. The exact number of required dishes will depend on the transfection efficiency and expression level. The sensor and cpVenus are expressed from CMV promoters on high-copy plasmids. When expressed in HEK293T cells, an efficient transfection of 4 × 10 cm dishes typically yields enough sensor or cpVenus protein for purification and calibration. Alternatively, stable cell lines can be generated (*see* Subheading 3.2).
2. We have successfully used lipid, calcium phosphate, and nucleofection approaches for transient transfection in HEK293T cells. We have found that high-quality, maxi-prepped plasmid DNA is optimal for obtaining high-efficiency transfections.
3. For the generation of sensor- and cpVenus-coated beads, it is most straightforward to express either the cytoplasmic or unlocalized plasmid versions. Sensor and cpVenus expressed without specific localization sequences predominantly reside in the cytoplasm.
4. The pH of the 2× HBS is critical for achieving a high rate of transfection. We have had success by adjusting to pH 7.1. We recommend preparing 3–4 solutions that range from pH 7.05 to 7.15 and first testing each one on a small scale with an eGFP plasmid to determine the optimal pH for transfection.
5. The lysate may need to be transferred to a shatter-proof centrifuge tube, depending on composition of the conical tube material. If using a fixed-angle rotor, an adaptor for conical tubes may be used as well.
6. We usually perform a Bradford assay [42] using the 5× BioRad Protein Assay™ following manufacturer's directions and BSA standard curve. In summary, the 5× BioRad reagent is freshly diluted to 1× in water, and 1 mL is added to a spectrophotometer cuvette. Add 2 μL of lysate, or 0.5% NETN buffer for the blank, to the reagent in the cuvette. Invert with parafilm to mix and immediately read absorbance at 595 nm. Interpolate absorbance measurement to BSA standard curve to obtain mg/mL of total protein in the lysate.
7. Typically, we obtain 20–50 mg of total protein from each lysate.
8. The sensor and cpVenus proteins encode N-terminal Flag-HA epitope tags and so will bind to the anti-Flag beads. These epitope tags follow the localization sequences and are connected to the sensor or cpVenus coding region with a flexible linker.

9. The exact values used for voltages are specific to every instrument and may take some time and sample to figure out for each instrumental setup. We suggest defining the setup prior to each new sample type, e.g., cell type, beads, etc. Suggested starting values for analyzing the anti-Flag magnetic beads include FSC-A (log), 50; SSC-A (log), 100; FL1-A (log), 250; and Violet-2A (log), 275.
10. The specific fluorescence filters denoted here for detection of emission are critical for taking advantage of the two distinct fluorescence peaks in the sensor and for ratiometric measurements.
11. Depending on instrumentation, it may be necessary to frequently clean the nozzle between samples to prevent clogs in the flow cell.
12. Confirm by checking for each condition that the gate is transferred and appropriately drawn such that it includes the correct cell population.
13. Confirm that a relatively equal number of beads (~500 events) are being evaluated in FL across all experimental conditions, excluding the nonfluorescent control sample.
14. The derived parameter function is used to obtain the 488/405 nm measurement per event, which is mathematically distinct from taking the average 488 nm fluorescence of the population and dividing by the average 405 nm fluorescence of the same population.
15. It is appropriate to use the geometric mean of this derived ratio as the fluorescence value for each experimental condition because fluorescence measurements are log-amplified.
16. This protocol represents a general framework that can be adapted to different cell types and for measurements in various subcellular compartments.
17. We describe a protocol for Lipofectamine 2000™, but many other methods to express exogenous DNA in mammalian cells will work here including other lipid-based approaches, calcium phosphate, viral transduction, electroporation, and nucleofection.
18. An N-terminal fusion of the SV40 nuclear localization sequence (PKKKRKV), connected via a flexible linker, targets the sensor and cpVenus proteins to the nucleus.
19. Do not leave cells out of the incubator for over 10 min as this may negatively affect their health.
20. We have found that MEM media works most consistently with nicotinamide riboside treatments. FK866 treatments can work in either MEM- or DMEM-based media.

21. Incubation longer than 18 h with FK866 results in dramatic NAD^+ depletion and compromised health of cells. Once cells are unhealthy, it is difficult to properly evaluate sensor responses and not advised.
22. From here onward, contamination of the cell culture is no longer a consideration, and cells can be prepared for analysis outside of the biosafety cabinet if needed.
23. HEPES is necessary in the media to buffer the cell suspension during flow analysis, which is typically performed on the bench outside of an incubator.
24. Phenol red will not interfere with the flow analysis because cells are diluted in sheath buffer during the analysis. Including serum in the media and keeping the cells on ice help to prevent cells from clumping.
25. For HEK293T cells, our suggested starting voltages are FSC-A (linear), 250; SSC-A (linear), 300; FL1-A (log), 250; and Violet-2A (log), 275.
26. For the untransfected sample, confirm that cells appear in P1 and P2 but not in P3 (Fig. 3b, gray population).

Acknowledgments

This work was supported by funding from the Hillcrest Committee Pilot Project Award and NIH DP2GM126897 and P30CA069533 to X.A.C. and The Pew Charitable Trusts to M.S.C. NAD^+ sensors which are available to the academic research community under a material transfer agreement with Oregon Health & Science University (OHSU). The authors are listed as inventors on patent PCT/US15/62003 for the NAD^+ sensor.

References

1. Chambon P, Weill JD, Mandel P (1963) Nicotinamide mononucleotide activation of new DNA-dependent polyadenylic acid synthesizing nuclear enzyme. Biochem Biophys Res Commun 11:39–43
2. Imai S, Armstrong CM, Kaeberlein M, Guarente L (2000) Transcriptional silencing and longevity protein Sir2 is an NAD-dependent histone deacetylase. Nature 403:795–800
3. Hottiger MO, Hassa PO, Lüscher B, Schüler H, Koch-Nolte F (2010) Toward a unified nomenclature for mammalian ADP-ribosyltransferases. Trends Biochem Sci 35:208–219
4. Gupte R, Liu Z, Kraus WL (2017) PARPs and ADP-ribosylation: recent advances linking molecular functions to biological outcomes. Genes Dev 31:101–126
5. Yang Y, Sauve AA (2016) NAD^+ metabolism: bioenergetics, signaling and manipulation for therapy. Biochim Biophys Acta 1864:1787–1800
6. Holzer H, Lynen F, Schultz G (1956) Determination of diphosphopyridine nucleotide/reduced diphosphopyridine nucleotide quotient in living yeast cells by analysis of constant alcohol and acetaldehyde concentrations. Biochem Z 328:252–263

7. Bucher T, Klingenberg M (1958) Wege des Wasserstoffs in der lebendigen Organisation. Angew Chem 70:552–570
8. Williamson DH, Lund P, Krebs HA (1967) The redox state of free nicotinamide-adenine dinucleotide in the cytoplasm and mitochondria of rat liver. Biochem J 103:514–527
9. Berger F, Lau C, Dahlmann M, Ziegler M (2005) Subcellular compartmentation and differential catalytic properties of the three human nicotinamide mononucleotide adenylyltransferase isoforms. J Biol Chem 280:36334–36341
10. Mori V, Amici A, Mazzola F, Di Stefano M, Conforti L, Magni G, Ruggieri S, Raffaelli N, Orsomando G (2014) Metabolic profiling of alternative NAD biosynthetic routes in mouse tissues. PLoS One 9:e113939
11. Zhang X, Kurnasov OV, Karthikeyan S, Grishin NV, Osterman AL, Zhang H (2003) Structural characterization of a human cytosolic NMN/NaMN adenylyltransferase and implication in human NAD biosynthesis. J Biol Chem 278:13503–13511
12. Lau C, Dölle C, Gossmann TI, Agledal L, Niere M, Ziegler M (2010) Isoform-specific targeting and interaction domains in human nicotinamide mononucleotide adenylyltransferases. J Biol Chem 285:18868–18876
13. Di Stefano M, Galassi L, Magni G (2010) Unique expression pattern of human nicotinamide mononucleotide adenylyltransferase isozymes in red blood cells. Blood Cells Mol Dis 45:33–39
14. Yang H, Yang T, Baur JA, Perez E, Matsui T, Carmona JJ, Lamming DW, Souza-Pinto NC, Bohr VA, Rosenzweig A, de Cabo R, Sauve AA, Sinclair DA (2007) Nutrient-sensitive mitochondrial NAD+ levels dictate cell survival. Cell 130:1095–1107
15. Dölle C, Niere M, Lohndal E, Ziegler M (2010) Visualization of subcellular NAD pools and intra-organellar protein localization by poly-ADP-ribose formation. Cell Mol Life Sci 67:433–443
16. Pittelli M, Formentini L, Faraco G, Lapucci A, Rapizzi E, Cialdai F, Romano G, Moneti G, Moroni F, Chiarugi A (2010) Inhibition of nicotinamide phosphoribosyltransferase: cellular bioenergetics reveals a mitochondrial insensitive NAD pool. J Biol Chem 285:34106–34114
17. Cambronne XA, Stewart ML, Kim D, Jones-Brunette AM, Morgan RK, Farrens DL, Cohen MS, Goodman RH (2016) Biosensor reveals multiple sources for mitochondrial NAD+. Science 352:1474–1477
18. VanLinden MR, Dölle C, Pettersen IK, Kulikova VA, Niere M, Agrimi G, Dyrstad SE, Palmieri F, Nikiforov AA, Tronstad KJ, Ziegler M (2015) Subcellular distribution of NAD+ between cytosol and mitochondria determines the metabolic profile of human cells. J Biol Chem 290:27644–27659
19. Nikiforov A, Dölle C, Niere M, Ziegler M (2011) Pathways and subcellular compartmentation of NAD biosynthesis in human cells: from entry of extracellular precursors to mitochondrial NAD generation. J Biol Chem 286:21767–21778
20. Hikosaka K, Ikutani M, Shito M, Kazuma K, Gulshan M, Nagai Y, Takatsu K, Konno K, Tobe K, Kanno H, Nakagawa T (2014) Deficiency of nicotinamide mononucleotide adenylyltransferase 3 (nmnat3) causes hemolytic anemia by altering the glycolytic flow in mature erythrocytes. J Biol Chem 289:14796–14811
21. Hung YP, Albeck JG, Tantama M, Yellen G (2011) Imaging cytosolic NADH-NAD(+) redox state with a genetically encoded fluorescent biosensor. Cell Metab 14:545–554
22. Bilan DS, Matlashov ME, Gorokhovatsky AY, Schultz C, Enikolopov G, Belousov VV (2014) Genetically encoded fluorescent indicator for imaging NAD(+)/NADH ratio changes in different cellular compartments. Biochim Biophys Acta 1840:951–957
23. Zhao Y, Hu Q, Cheng F, Su N, Wang A, Zou Y, Hu H, Chen X, Zhou HM, Huang X, Yang K, Zhu Q, Wang X, Yi J, Zhu L, Qian X, Chen L, Tang Y, Loscalzo J, Yang Y (2015) SoNar, a highly responsive NAD+/NADH sensor, allows high-throughput metabolic screening of anti-tumor agents. Cell Metab 21:777–789
24. Zhu XH, Lu M, Lee BY, Ugurbil K, Chen W (2015) In vivo NAD assay reveals the intracellular NAD contents and redox state in healthy human brain and their age dependences. Proc Natl Acad Sci U S A 112:2876–2881
25. Baird GS, Zacharias DA, Tsien RY (1999) Circular permutation and receptor insertion within green fluorescent proteins. PNAS 96:11241–11246
26. Nagai T, Ibata K, Park ES, Kubota M, Mikoshiba K, Miyawaki A (2002) A variant of yellow fluorescent protein with fast and efficient maturation for cell-biological applications. Nat Biotechnol 20:87–90
27. Sanford L, Palmer A (2017) Recent advances in development of genetically encoded fluorescent sensors. Methods Enzymol 589:1–49
28. Rodriguez EA, Campbell RE, Lin JY, Lin MZ, Miyawaki A, Palmer AE, Shu X, Zhang J, Tsien RY (2017) The growing and glowing toolbox of fluorescent and photoactive proteins. Trends Biochem Sci 42:111–129

29. Gajiwala KS, Pinko C (2004) Structural rearrangement accompanying NAD^+ synthesis within a bacterial DNA ligase crystal. Structure 12:1449–1459
30. Lahiri SD, Gu RF, Gao N, Karantzeni I, Walkup GK, Mills SD (2012) Structure guided understanding of NAD^+ recognition in bacterial DNA ligases. ACS Chem Biol 7:571–580
31. Nagai T, Sawano A, Park ES, Miyawaki A (2001) Circularly permuted green fluorescent proteins engineered to sense Ca2+. PNAS 98:3197–3202
32. Tian L, Hires SA, Mao T, Huber D, Chiappe ME, Chalasani SH, Petreanu L, Akerboom J, McKinney SA, Schreiter ER, Bargmann CI, Jayaraman V, Svoboda K, Looger LL (2009) Imaging neural activity in worms, flies and mice with improved GCaMP calcium indicators. Nat Methods 6:875–881
33. Akerboom J, Chen TW, Wardill TJ, Tian L, Marvin JS, Mutlu S, Calderón NC, Esposti F, Borghuis BG, Sun XR, Gordus A, Orger MB, Portugues R, Engert F, Macklin JJ, Filosa A, Aggarwal A, Kerr RA, Takagi R, Kracun S, Shigetomi E, Khakh BS, Baier H, Lagnado L, Wang SS, Bargmann CI, Kimmel BE, Jayaraman V, Svoboda K, Kim DS, Schreiter ER, Looger LL (2012) Optimization of a GCaMP calcium indicator for neural activity imaging. J Neurosci 32:13819–13840
34. Chen TW, Wardill TJ, Sun Y, Pulver SR, Renninger SL, Baohan A, Schreiter ER, Kerr RA, Orger MB, Jayaraman V, Looger LL, Svoboda K, Kim DS (2013) Ultrasensitive fluorescent proteins for imaging neuronal activity. Nature 499:295–300
35. Zhao Y, Araki S, Wu J, Teramoto T, Chang YF, Nakano M, Abdelfattah AS, Fujiwara M, Ishihara T, Nagai T, Campbell RE (2011) An expanded palette of genetically encoded Ca^{2+} indicators. Science 333:1888–1891
36. Belousov VV, Fradkov AF, Lukyanov KA, Staroverov DB, Shakhbazov KS, Terskikh AV, Lukyanov S (2006) Genetically encoded fluorescent indicator for intracellular hydrogen peroxide. Nat Methods 3:281–286
37. Grynkiewicz G, Poenie M, Tsien RY (1985) A new generation of Ca2+ indicators with greatly improved fluorescence properties. J Biol Chem 260:3440–3450
38. Sakaguchi R, Endoh T, Yamamoto S, Tainaka K, Sugimoto K, Fujieda N, Kiyonaka S, Mori Y, Morii T (2009) A single circularly permuted GFP sensor for inositol-1,3,4,5-tetrakisphosphate based on a split PH domain. Bioorg Med Chem 17:7381–7386
39. Zhao Y, Jin J, Hu Q, Zhou HM, Yi J, Yu Z, Xu L, Wang X, Yang Y, Loscalzo J (2011) Genetically encoded fluorescent sensors for intracellular NADH detection. Cell Metab 14:555–566
40. Casey JR, Grinstein S, Orlowski J (2010) Sensors and regulators of intracellular pH. Nat Rev Mol Cell Biol 11:50–61
41. Anderson BM, Anderson CD (1963) The effect of buffers on nicotinamide adenine dinucleotide hydrolysis. J Biol Chem 238:1475–1478
42. Bradford MM (1976) A rapid and sensitive method for the quantitation of microgram quantities of protein utilizing the principle of protein-dye binding. Anal Biochem 72:248–254